HEAT TRANSFER AND HUMIDITY EFFECTS DURING COLD DENSE GAS DISPERSION

by

Robert N. Meroney[1]

and

David E. Neff[2]

Prepared for Submission to

Third Symposium on Heavy Gases and Risk Assessment
12-13 November 1984
Wissenschaftszentrum, Bonn, F.R.G.

Fluid Mechanics and Wind Engineering Program
Department of Civil Engineering
Colorado State University
Fort Collins, CO 80523

[1] Professor-in-charge, FMWE Program
Civil Engineering Department

[2] Research Associate
Civil Engineering Department

CEP84-85RNM-DEN3
Revised February 1985

HEAT TRANSFER AND HUMIDITY EFFECTS DURING COLD DENSE GAS DISPERSION

Robert N. Meroney and
David E. Neff
Fluid Mechanics and Wind Engineering Program
Civil Engineering Department
Colorado State University
Fort Collins, CO 80523 USA

ABSTRACT. Wind-tunnel concentration data were obtained for continuous area releases of ambient temperature Freon-air mixtures, cold nitrogen, cold carbon dioxide and cold methane clouds. Wind-tunnel results were compared to a computer model simulation. Heat transfer and humidity effects on model concentration distributions were significant for methane plumes when surface Richardson numbers, Ri_*, were large (i.e., low wind speed and high boiloff rate conditions). At field scales heat transfer and humidity still play a role in the dispersion of calculated methane spills, but plume dilution and lift-off are not as exaggerated as for the model methane cases.

1. INTRODUCTION

Storage and transport of flammable hydrocarbon fuels such as liquefied natural gas (LNG), ethane, propane, and butane (LPG) may result in inadvertent releases into the atmosphere. At ambient temperatures these liquids rapidly boil and form cold gas clouds that will remain negatively buoyant unless the cloud is subjected to heat transfer or warming due to condensation of water vapor. Earlier experiments by the authors have dealt with the behavior of ambient temperature dense gas clouds released instantaneously (Meroney and Lohmeyer, 1981, 1984a, 1984b), continuously or over finite intervals (Meroney and Neff, 1981, 1982), continuously in the presence of surface obstacles (Kothari and Meroney, 1982, 1984), and continuously while interacting with water spray curtains (Heskestad et al, 1983; Meroney, et al, 1984).

A generalized box-type numerical model (Meroney and Lohmeyer, 1984) and a depth-integrated slab-type numerical model (Meroney 1984a, 1984b) were developed to evaluate the dense gas dispersion. Adjustable constants in the models were chosen to maximize the agreement between the models and the laboratory ambient temperature gas data. The models contained algorithms to account for the effects of surface heat transfer and water vapor condensation; however, the accuracy of these expressions was unknown.

Since the previous experiments did not illuminate the influence of thermal effects on plume spreading or mixing behavior a new series of experiments were performed to study the effect of heat transfer and humidity on cold dense cloud dispersion. The performance of the integrated-depth slab model when compared to the cold gas laboratory data is the subject of this paper.

2. COLD DENSE GAS EXPERIMENTS

The cold dense plume measurement program was designed to provide a basis for the analysis of heat transfer effects on plume dispersion and to assist in the development of and verification of numerical models. Source gas mixtures were prepared to provide gases which were all initially heavy; but they were either ambient temperature, cold with molar specific heat equal to that of air, or cold with specific heat capacity greater than that of air. Thus one could evaluate whether dilution and plume dimensions resulted from adiabatic entrainment, heat transfer effects, or unbalanced thermal expansion. A total of 43 experiments were performed such that the buoyancy length scale, l_b, ranged from 0.7 to 9.2; the Richardson number, Ri_*, lay between 7.7 and 33.1; the Reynolds number, Re, varied from 9.9 to 22.2; and the Grashoff number fell between 0 and 210.

The cold gas experiments were modeled in the Environmental Wind Tunnel (EWT) at Colorado State University. This atmospheric boundary-layer wind tunnel has a test section 3.66 m wide, 2.28 m tall, and 17.0 m long. Vortex generators and a wall trip at the test-section entrance produced a boundary layer about one meter deep at the experiment location 10.0 m downwind of the entrance.

A constant area source was mounted flush with the floor of the EWT. Two heavy ambient temperature and three cooled gases were released continuously from the source. A heat exchanger, Figure 1, was used to establish the proper thermal conditions of the source gases. The heat exchanger used nitrogen as a cooling fluid. A pool of liquid nitrogen was maintained around the source gas plenum, so that little if any source gas heating would occur before the gas became exposed to the ambient atmosphere. The source gas was cooled in a gas-to-gas counterflow heat exchanger. Temperatures were regulated by adjusting coolant gas temperatures and flow rate, such that release temperatures were set within $\pm 5^{o}$K. All source gases contained a known percentage of a hydrocarbon tracer. An oil smoke was used to define visually ambient temperature gas plume behavior, while cold gas plume boundaries could be observed as a result of background humidity condensation within the plume. Correlation of plume outlines with concentration isopleths suggests the smoke edges reflect a concentration near 0.1%.

The approach-wind velocity profile, reference-wind speed conditions, and turbulence were measured with a Thermo-systems 1050 anemometer and 1212 hot-film probe. Multipoint calibration procedures suggest that velocities were measured within five to ten percent of their actual values. A thermocouple multiplexer (Model Digitrend 22) monitored up to 45 copper/constantan thermocouples once each minute

during each experiment.

Average concentrations were measured at 81 stations for each simulated spill. The floor in the vicinity of the plumes was always flat and smooth with no obstacles to cause wake effects. To obtain a series of vertical profiles, experiments were replicated up to five times, and only data at or upwind of any concentration probe rake was considered accurate. The replications provided redundant data that defined concentration variability between test runs. Samples were drawn from the tunnel in 50 sample sets over a period of five minutes at a rate of about six cc/min. Such sampling times are equivalent to 10-20 minute averages at field scales. Individual samples were then evaluated for tracer gas concentration by a flame-ionization detector in a gas chromatograph (Hewlett Packard Model 5710A). The error in measured concentration is imposed by the detector sensitivity, source strength and sampling uncertainties, and the background concentration of tracer within the wind tunnel. Background concentrations were measured and subtracted from all data; hence, final model concentrations are accurate to $\pm 10\%$ over most of the detection range. The cold gas experiments and data are discussed in greater detail in the report by Andriev, Neff, and Meroney (1983) and the paper by Meroney and Neff (1984).

All concentrations are expressed in terms of methane equivalent concentrations. The methane equivalent values must be used to avoid making interplume comparisons based on different source molar flux rates associated with different initial temperature conditions. (See Neff and Meroney, 1982).

3. A DEPTH-AVERAGED NUMERICAL MODEL

A wind-tunnel calibrated, depth-integrated numerical model was used to calculate the behavior of cold gas clouds released into the atmosphere at ground level. The model (DENS20) is time dependent, quasi-three-dimensional, and permits cloud heating from below and entrainment of moist air. The model does not depend upon the Boussinesq assumption, but it does require the hydrostatic assumption. In Meroney (1984a) the model was verified by reproducing plume shape and concentration decay with distance and time for comparative cases from the Porton Downs field tests (Picknett, 1981), the China Lake field tests (Koopman et al, 1982) and these cold gas laboratory tests on dense gas behavior. In Meroney (1984b) the same model was used to perform numerical experiments on the character of upwind motion and head wave breaking during transient LNG spills; the evidence for gravity waves on the cloud upper surface; source behavior during instantaneous, finite time, and continuous gas release; and the shape of transient ignition zones.

The plume properties (height, width, density, velocities, enthalpy, and concentration) are treated explicitly in their dependence on the downwind direction and on time, but they are averaged over crosswind section. The model consists of six coupled, partial differential equations which solve for plume width and section averaged height, density, enthalpy, lateral and longitudinal velocities, and mass fraction. The equations were developed in a difference form using an

implicit, second-upwind-difference, donor-cell approach. The difference equations are solved by sequential use of the Thomas algorithm.

Formulae for the vertical and horizontal entrainment speeds, w_e and v_e, are based on perturbations of forms suggested by Edisvik (1980) and Ermak et al (1982). Unspecified constants are determined by calibration of the model with laboratory data from Meroney and Lohmeyer (1982) and Neff and Meroney (1982). Expressions in the enthalpy conservation equation adjust for heat initially released when the cold plume entrains water vapor, but which is subsequently re-evaporated when the temperature of the plume exceeds ambient dew point. Surface heat transfer coefficients are predicted by an algorithm suggested by Leovy (1969) for mixed free and forced convection in the atmosphere. Alternative values for fully forced or fully free convection can also be used.

Readers interested in the details of model formulation are referred to Meroney (1984a) or Meroney and Lohmeyer (1982). Other depth-averaged type models are described by Colenbrander (1980), Zeman (1982), and Morgan, Morris, and Ermak (1983).

4. BEHAVIOR OF COLD DENSE GAS PLUMES

Initially, all of the continuous cold plumes exhibited rapid horizontal spreading caused by the excess hydrostatic head of the cloud. This resulted in a low wide plume, the effect being more pronounced at low wind speeds. In instances of low and moderate wind speed, the plumes extended upwind, but, as the gases lost their initial upwind momentum, they were rolled back over and around the source. A consequence of the velocity reversal of gas upwind from the source was the generation of a horseshoe shaped vortex, which bounded the laterally parabolic gas cloud.

Surface heating of the cold plumes and heat from condensation of entrained water vapor with the air reduced the plumes' negative buoyancy. The result was a decrease in the instantaneous Richardson number thereby enhancing both dispersion by atmospheric turbulence and the subsequent downwind advection of the plume. As the buoyancy became positive for the methane plumes and the plume less stably stratified, rapid vertical growth occurred.

4.1 General Appearance of the Cold Gas Plumes

Typical surface concentration isopleths are plotted in Figures 2 to 4 for isothermal, cold nitrogen, and cold carbon dioxide gases when l_b = 4 cm. On each curve the visual extent of the cloud associated with smoke or water droplets is indicated by a dashed line. The plumes continue to grow laterally even after the hydrostatically driven spread velocity is nearly zero. The plume lateral growth rates approach values associated with mixing due to background ambient turbulence.

4.2 Vertical Concentrations

Vertical concentration profiles were made at x = 0.3 to 2.4 m downwind of the source on the plume centerline. In no case did we see the flat, well-mixed regions with the plumes proposed by several authors to result from thermal convection. Instead the profiles decay in either a Gaussian or exponential manner. Ambient temperature Freon-air mixtures, cold nitrogen, and cold carbon dioxide plumes always remained negatively buoyant; thus, the maximum vertical extent of the plumes rarely exceeded z = 3 cm at x = 3 m. The stable stratification in the plumes suppressed vertical mixing, so vertical growth followed the character of a Pasquill-Gifford F category plume (See Figure 5).

The cold methane plumes became positively buoyant after contact with the warm wooden wind-tunnel floor increased plume temperatures. Thus the methane plume heights grew rapidly within 20 cm of the source (See Figure 6). Vertical growth rates appeared to approach Pasquill-Gifford A category rates (unstable atmosphere). Indeed the plume appeared visually to loft above the floor; although the vertical concentration profiles never showed a maximum above the ground.

4.3 Temperature Profiles

Temperatures measured are also displayed on Figures 5 and 6. Local plume concentrations may be compared with local temperatures as noted on Figure 7. Predicted variations for dry adiabatic and humid adiabatic mixing are noted. These curves are independent of any entrainment model and assume only adiabatic mixing of constant property ideal gases. Predicted variations including heat transfer effects are provided by the depth averaged numerical box model. Re-evaporation of condensed water vapor results in the sudden change in slope or kinks observed on the figure. Surface heat transfer produces higher temperatures at lower dilution levels.

4.4 Concentration Results

Heat transfer effects may be readily observed in the relative mixing rates of the various plumes and the resultant variation in centerline concentration with distance. Figures 8 through 10 show centerline methane-equivalent concentrations, C, versus downwind distance, x for selected runs. The isothermal runs are essentially coincident. Cold plumes did not produce similar behavior. They generally arranged themselves in order of initial temperature, where a lower source temperature subsequently leads to faster dilution rates. An interesting exception in the cold carbon dioxide plume where the large specific heat capacity results in centerline concentrations slightly above any ambient temperature counterpart.

An alternative data presentation is provided in Figure 11, where a dimensionless concentration, $K = [T_o/T_a][C/(1-C)][U_R L_R^2/Q]$, suggested by Neff and Meroney (1982) is plotted versus downwind distance x. This plot automatically normalizes for source variations in volume flow rate

or temperature. A band of data associated with isothermal experiments falls above the methane data. Model methane plumes would produce such values if heat transfer effects were absent. The cold methane plumes dilute faster as buoyancy length scale increases.

5. COMPUTED BEHAVIOR OF COLD DENSE GAS PLUMES

Calculations with the depth-integrated numerical model were performed over the source area, wind speed, and roughness conditions examined experimentally. When the gas parcels remain negatively buoyant throughout their dispersion history the slab model faithfully predicts concentration decay and plume growth. For situations where parcel densities fall below ambient densities the model cannot predict the tendency for the cloud to lift off and narrow.

Included on Figures 8, 9, 10, and 11 are the cloud values predicted by the numerical model. Agreement is generally good, the inter-test variations seen in the data are reproduced in the same sense by the numerical model. In particular the mixed convection algorithm suggested by Leovy (1969) seems to be appropriate for mixing of cold gas plumes.

One advantage of a numerical model is that various assumptions and submodels can be switched on and off to test their influence. Figure 12 reflects the effects of different surface heat transfer assumptions on a cold methane plume released under conditions equivalent to Run 3 (l_b = 5). Under model conditions the perturbation effects of heat transfer and humidity are significant. Thermal effects result in 50% lower concentrations and a 40% narrower plume at a distance downwind of one meter. Latent heat release only slightly perturbs the adiabatic dry plume results; thus surface heat transfer effects are dominant.

6. CONCLUSIONS

A large data base detailing heavy gas plume temperatures and concentrations was obtained in an atmospheric boundary-layer wind tunnel. Releases included ambient temperature and cold gas plumes. Heat transfer and humidity effects on model concentration distributions were significant for methane plumes when the buoyancy length scales or Richardson numbers are large. Ambient temperature mixtures and heavier molecular weight cold simulants always produced higher surface concentrations than the buoyant methane plumes. At field scales heat transfer and humidity are expected to still play a role in the dispersion of methane spill cases, but plume dilution and lift-off will not be as exaggerated as for the model cases.

The depth-integrated model (DENS20) was seen to reproduce the essence of dense cloud behavior for isothermal or cold dense clouds. The program is reasonably simple (350 lines of Fortran code including print and plot statements), is fast (320 time steps forward in 110 sec cpu time on a CDC CYBER 172 computer), and does not occupy a large amount of computer memory (a version of the program written in BASIC occupies less than 64 k on an IBM PC microcomputer).

ACKNOWLEDGEMENTS

The authors wish to acknowledge support from the Gas Research Institute, Chicago, Illinois, U.S.A., through Contract No. 5014-352-0203.

LIST OF SYMBOLS

Symbol	Definition
g'	Modified gravitational constant, $g(\Delta\rho/\rho)$
Gr	Grashoff number, $g H_o^3 \Delta T / \nu^2$
H	Cloud depth
K	Dimensionless concentration coefficient
l_b	Buoyancy length scale, $g'Q/U_R^3$
Q	Source strength
Re	Reynolds number, $(g'H_o^3)^{1/2}/\nu$
Ri_*	Richardson number, $g'H_o\rho_o/u_*^2$
SG	Specific gravity, ρ_o/ρ_a
T	Temperature
U	Velocity
u_*	Friction velocity
w_e, v_e	Entrainment velocities
x,y,z	Coordinates
ρ	Density
ν	Kinematic viscosity
ϕ	Volumetric concentration
ϕ	Humidity

Subscripts	
o	Source conditions
a	Ambient conditions
R	Reference conditions

REFERENCES

Andriev, G., Neff, D.E., and Meroney, R.N. (1983), Heat Transfer Effects During Cold Dense Gas Dispersion, Gas Research Institute Report 83/0082, 200 p.

Colenbrander, G.W. (1980), °A Mathematical Model for the Transient Behaviour of Dense Vapour Clouds', Proceedings 3rd Int. Symp. on Loss Prevention and Safety Promotion in the Process Industries, Basel, Switzerland, 29 pp.

Eidsvik, K.J. (1980), ° A Model for Heavy Gas Disperion in the Atmosphere', Atmospheric Environment, Vol. **14**, 769-777.

Ermak, D.L., Chan, S.T., Morgan, D.L., and Morris, L.K. (1982), °A Comparison of Desne Gas Dispersion Model Simulations with Burro Series LNG Spill Test Results', Journal of Hazardous Materials, Vol. **6**, Nos. 1 and 2, 43-84.

Heskestad, G., Meroney, R.N., Kothari, K.M., and Neff, D.E. (1983), °Effectiveness of Water Spray Curtains in Dispersing LNG Vapor Clouds', Proceedings of the American Gas Association, Transmission

Conference, Paper 83-T-69, 1-4 May 1983, Seattle, Washington, pp. T-169 to T-183.

Koopman, R.P., Cederwall, R.T., Ermak, D.L., Goldwire, H.C. Jr., Hogan, W.J., McClure, J.W., McRAe, T.G., Moran, D.L., Rodean, H.C., and Shinn, J.H. (1982), 'Analysis of Burro Series 40 m^3 LNG Spill Experiments', Journal of Hazardous Materials, Vol. **6**, Nos. 1 and 2, 43-84.

Kothari, K.M. and Meroney, R.N. (1982), Accelerated Dilution of Liquified Natural Gas Plumes with Fences and Vortex Generators, Gas Research Institute Report 81/0074, 222 p.

Kothari, K.M. and Meroney, R.N. (1984), Liquified Natural Gas (LNG) Plume Interactions with Storage Tanks, Winter Annual Meeting, ASME, New Orleans, 13-15 December, 23 p.

Leovy, C.B. (1969), 'Bulk Transfer Coefficient for Heat Transfer', Journal of Geophysical Research, Vol. **74**, No. 13, 3313-3321.

Meroney, R.N. (1984a), 'Transient Characteristics of Dense Gas Dispersion; Part I: A Depth-Averaged Numerical Model', Journal of Hazardous Materials, Vol. ---, 29 p.

Meroney, R.N. (1984b), 'Transient Characteristics of Dense Gas Dispersion; Part II: Numerical Experiments on Dense Cloud Physics', Journal of Hazardous Materials, Vol. ---,22 p.

Meroney, R.N., Lohmeyer, A., and Plate, E.J. (1981), 'Model Investigations of the Spreading of Heavy Gases Released from an Instantaneous Source at the Ground', Air Pollution Modelling and Its Application, C. De Wispelaere, ed., Plenum Publishing Co., 433-448.

Meroney, R.N. and Lohmeyer, A. (1982), Gravity Spreading and Dispersion of Dense Gas Clouds Released Suddenly into a Turbulent Boundary Layer, Gas Research Institute Report 81/0025, 220 p.

Meroney, R.N. and Lohmeyer, A. (1984a), 'Prediction of Propane Cloud Dispersion by a Wind-Tunnel Calibrated Box Model', Journal of Hazardous Materials, Vol. **8**, 205-221.

Meroney, R.N. and Lohmeyer, A. (1984b), 'Statistical Characteristics of Instantaneous Dense Gas Clouds Released in an Atmospheric Boundary Layer Wind Tunnel', Journal of Boundary Layer Meteorology, Vol. **28**,1-22.

Meroney, R.N. and Neff, D.E. (1981), 'Physical Modeling of Forty Cubic Meter LNG Spills at China Lake, California', Air Pollution Modelling and Its Application, C. De Wispelaere, ed., Plenum Publishing Co., 16 p.

Meroney, R.N. and Neff, D.E. (1982), °Dispersion of Vapor from LNG Spills--Simulation in a Meteorological Wind Tunnel: Six Cubic Meter China Lake Spill Series', Journal of Wind Engineering and Industrial Aerodynamics, Vol. **10**, 1-19.

Meroney, R.N. and Neff, D.E. (1984), °Heat Transfer Effects During Cold Dense Gas Dispersion: Wind-Tunnel Simulation of Cold Gas Spills', Winter Annual Meeting, ASME, New Orleans, 13-15 December, 8 p.

Meroney, R.N., Neff, D.E., and Heskestad, G. (1984), °Wind-Tunnel Simulation of U.K. Health and Safety Executive Water Spray Curtain Dense Gas Dispersion Test', Journal of Boundary Layer Meteorology, Vol. **28**, 107-119.

Morgan, D.L. Jr., Morris, L.K., and Ermak, D.L. (1983), SLAB: A Time-Dependent Computer Model for the Dispersion of Heavy Gases Released in the Atmosphere, Lawerence Livermore National Laboratory Report UCRL-53383, 15 p.

Neff, D.E. and Meroney, R.N. (1982), The Behavior of LNG Vapor Clouds: Wind-Tunnel Tests on the Modeling of Heavy Plume Dispersion, Gas Research Institute Report 80/0145, 120 p.

Picknett, R.G. (1981), °Dispersion of Dense Gas Puffs Released in the Atmosphere at Ground Level', Atmospheric Environment, Vol. **15**, 509-525.

Zeman, O. (1982), °The Dynamics and Modeling of Heavier-than-air, Cold Gas Releases', Atmospheric Environment, Vol. **16**, No. 4, 741-751.

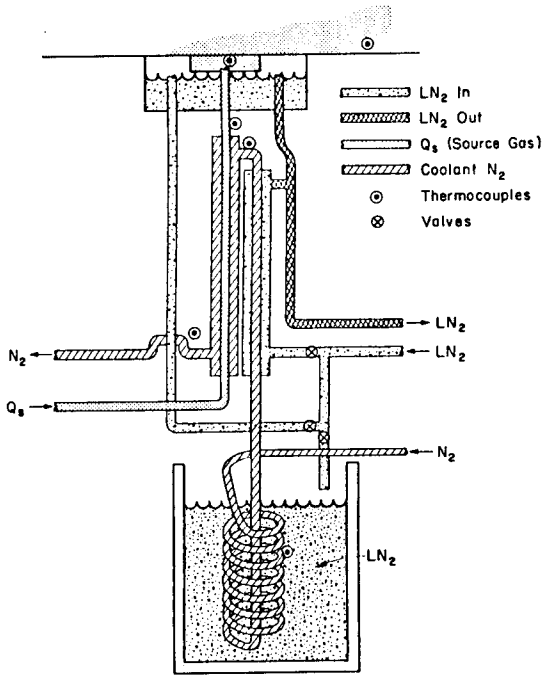

Figure 1 Schematic Diagram Cryogenic Heat Exchanger to Cool Source Gases and Plenum.

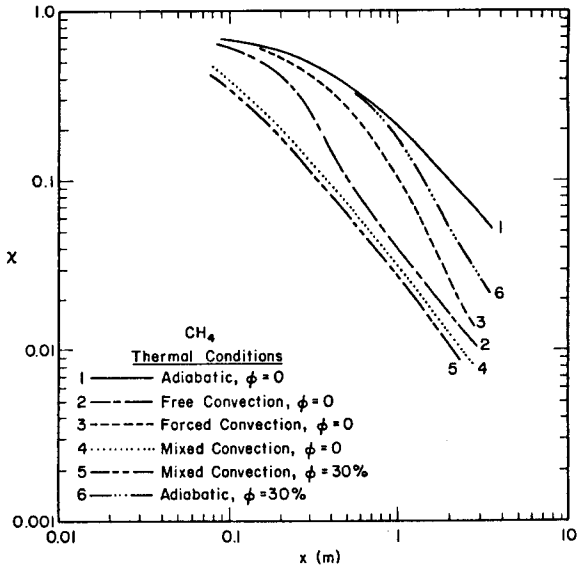

Figure 12 Centerline Surface Concentration Variation with Distance. Cold Methane Release, $T_0=111^\circ$, $\ell_b=4.0$ cm, Q=130 ccs, $u_*=1.85$ cm/sec, $z_0=0.0001$ m, Model for Various Thermal conditions.

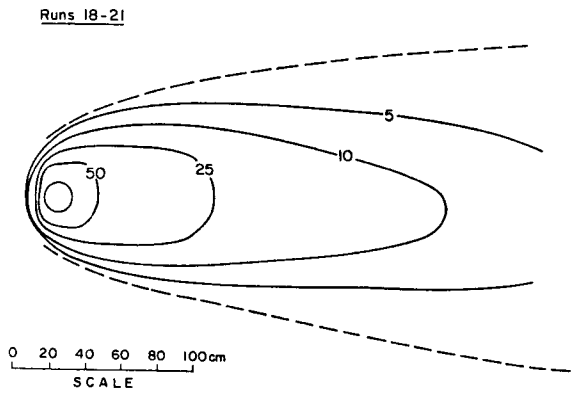

Figure 2 Surface Concentration Isopleths, Runs 18-21, Isothermal Gas, ℓ_b=4.0, Q=223 ccs, u_*=3.20 cm/s.

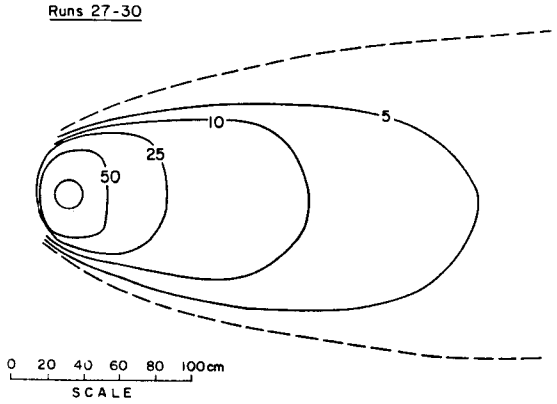

Figure 3 Surface Concentration Isopleths, Runs 27-30, Cold Nitrogen, ℓ_b=4.0, Q=223 ccs, u_*=3.20 cm/s.

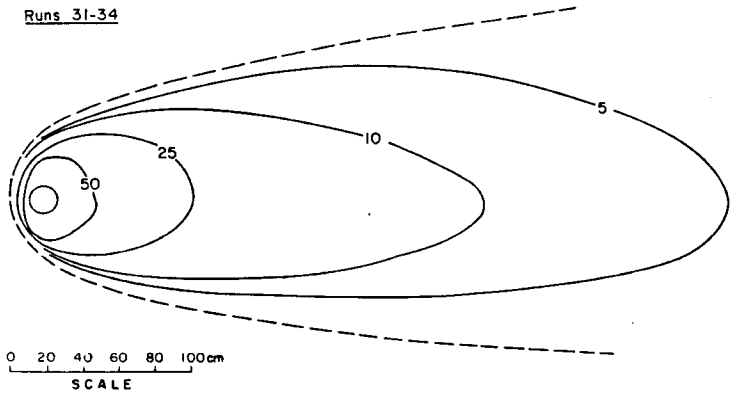

Figure 4 Surface Concentration Isopleths, Runs 31-34, Cold Carbon Dioxide, ℓ_b=3.9, Q=223 ccs, u_*=3.20 cm/s.

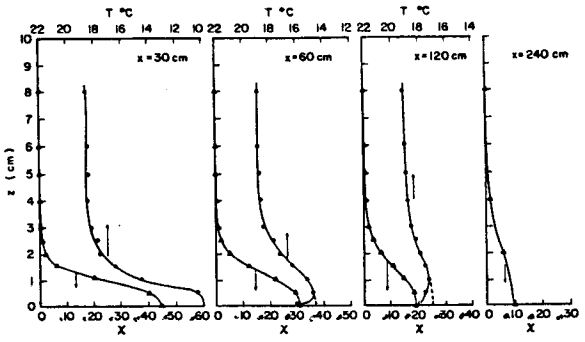

Figure 5 Vertical Temperature and Concentration Profiles, Runs 31-34, Cold Carbon Dioxide, ℓ_b=3.9, Q=223 ccs, u_*=3.20 cm/s.

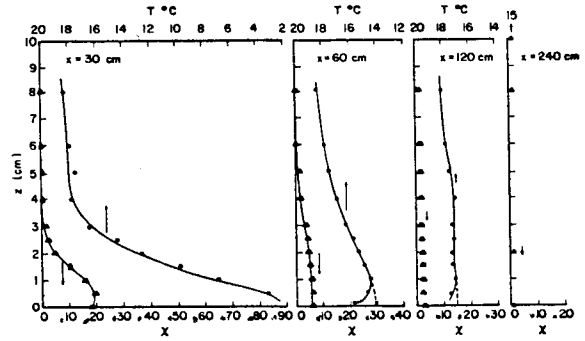

Figure 6 Vertical Temperature and Concentration Profiles, Runs 31-34, Cold Methane, ℓ_b=2.9, Q=130 ccs, u_*=1.85 cm/s.

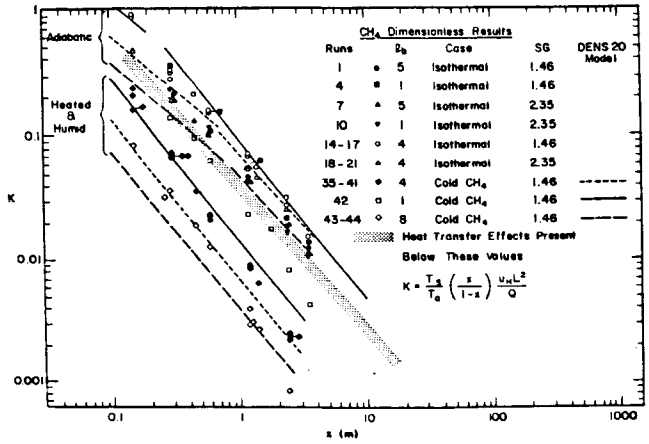

Figure 11 Dimensionless Concentration Coefficient Variation with Distance, Isothermal and Methane Runs, Numerical Prediction by DENS 20 Model. *During Runs 1-13 the wakes of sampling tube suspended over the cloud artificially reduced plume concentrations.

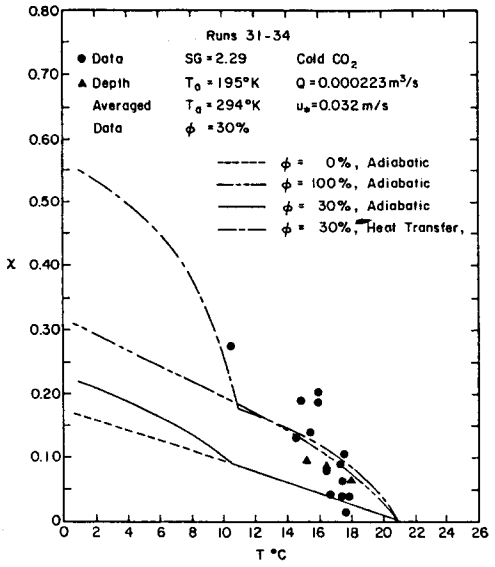

Figure 7 Concentration Against Temperature Measurements for Vertical Profile Stations, Runs 31-34, Cold Carbon Dioxide, ℓ_b=3.9, Q=223ccs, u_*=3.20 cm/s.

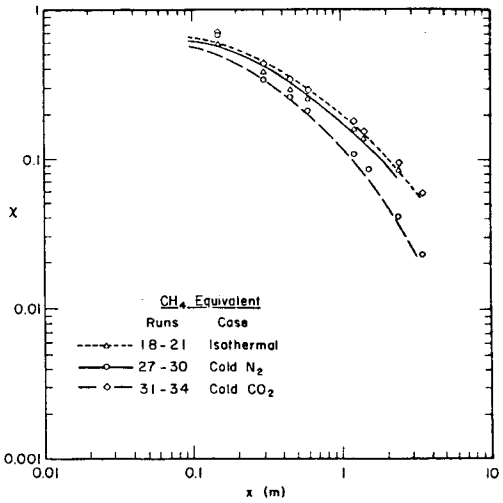

Figure 8 Concentration Decay with Down-wind Distance - Data and Numerical Predictions, Runs 18-21, 27-30, and 31-34, ℓ_b = 1 cm.

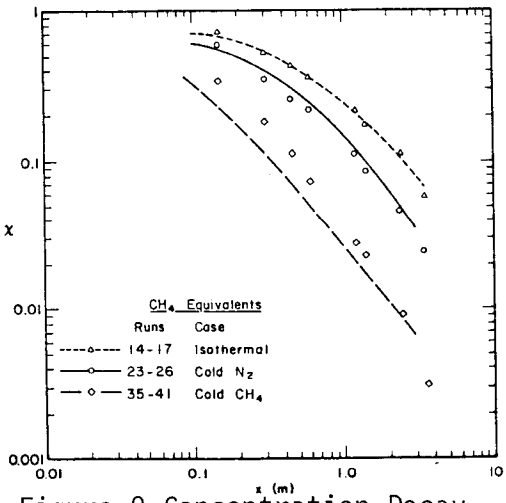

Figure 9 Concentration Decay with Down-wind Distance - Data and Numerical Predictions, Runs 14-17, 23-26, and 25-41, ℓ_b=4 cm.

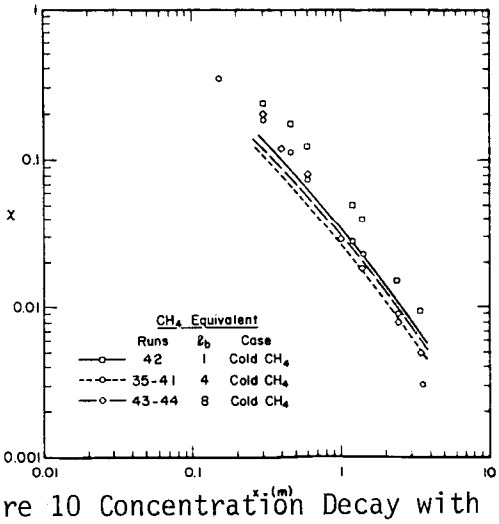

Figure 10 Concentration Decay with Down-wind Distance - Data and Numerical Predictions, Methane Runs ℓ_b=1, 4, and 8 cm.